SPECIATION AND LOCAL STRUCTURE IN ALKALI AND ALKALINE EARTH SILICATE GLASSES: CONSTRAINTS FROM ^{29}Si NMR SPECTROSCOPY

E. SCHNEIDER *, J.F. STEBBINS [†] and A. PINES

Department of Chemistry, University of California, Berkeley CA 94720; and Materials and Molecular Research Division, Lawrence Berkeley Laboratory, Berkeley CA 94720, USA

^{29}Si NMR spectroscopy provides important contributions to the understanding of silicate glass structure, as the resonance frequency is sensitive to several aspects of the local chemical environment (including intertetrahedral bond angles, bond distances, and number of bridging oxygens per silicon atom). New data on a series of binary alkali and alkaline earth glasses are presented which highlight the effects of composition, as well as the complications that can arise in the interpretation of spectra. In binary alkali silicate glasses, two partially resolved peaks may be observed, which are attributable to Si in sites with different numbers of bridging oxygens. These are present even in glasses which are almost certainly single, homogeneous phases. In alkaline earth and in aluminosilicate glasses, single, broad, often asymmetric resonances are found, whose linewidths span the frequency ranges of three or more structural species. Using a combination of slow sample spinning and non-spinning techniques, NMR spectra also provide data on local electronic symmetry, and indicate that silicon sites in glasses can be more symmetrical than those in crystalline materials.

1. Introduction

Silicate glasses are interesting not only because of their commercial usefulness and their occurrence in nature, but because they can be assumed to provide a snapshot view of the molten state. As a melt is quenched, the liquid structure at the glass transition temperature (T_g) is preserved. This quenched-in local structure has been observed in glassed by infrared and Raman spectroscopy, e.g. [1–8], X-ray and neutron scattering , e.g. [9–11], X-ray emission, e.g. [12], EXAFS and XANES spectroscopy, e.g. [13], and ^{29}Si magic angle spinning (MAS) nuclear magnetic resonance (NMR) spectroscopy, e.g. [14–27].

Most silicates contain silicon atoms bound to four oxygen atoms in a tetrahedral arrangement. These tetrahedra may be linked to each other by

* Current address: Physikalisches Institut, Teil 2, Universität Stuttgart, 7000 Stuttgart 80, West Germany
[†] To whom all correspondence should be addressed: Department of Geology, Stanford University, Stanford, CA 94305, USA.

shared oxygen atoms, with more polymerized structures having more oxygen atom bridges. The local degree of connectivity, a fundamental aspect of any structure, can thus be described in terms of $Q^n (0 \le n \le 4)$ species, where n is the number of bridging oxygen atoms per silicate tetrahedron. The dynamics and disorder present in a molten silicate cause the corresponding glass to have much less long-range order, and a wider variation in Si–O–Si bond angles and Si–O bond lengths than are present in crystalline materials. Although all evidence indicates that the tetrahedral units present in the crystal are also present in the glass, a range of species may be formed through reactions which take place in the melt (for $1 \le n \le 3$):

$$2Q^n = Q^{n-1} + Q^{n+1}. \tag{1}$$

A similar reaction may be written to illustrate the disordering of Al and Si distributions which occur during heat treatment or melting of many aluminosilicates [28]. A central question of glass structure concerns the extent of such speciation reactions, and their importance in controlling the physical and chemical properties of glassy and molten silicates.

NMR spectroscopy is very sensitive to the local electronic environment surrounding non-zero spin nuclei [29]. ^{29}Si NMR has proven particularly useful in investigations of aqueous (e.g. [30]), crystalline (e.g. [31]), glassy [15–27], and molten [32–33] silicate structure. Because both silicate speciation and geometric factors (such as Si–O–Si bond angles [34–38] and Si–O bond lengths [39]) influence ^{29}Si chemical shifts, NMR is potentially useful for characterizing several aspects of local silicate structure. However, interpretation of the ^{29}Si MAS NMR spectra of glasses is complicated by the fact that peaks are often an order of magnitude broader than those in the spectra of corresponding crystalline samples. At least in glasses containing only small amounts of paramagnetic impurities, wide lines are due to real distributions of structural variables ("heterogeneous broadening"), and thus reflect disordered amorphous structures.

Several studies have used isotropic chemical shifts, determined by magic angle spinning (MAS) NMR studies, to investigate the range of silicon environments in glasses of simple binary silicate composition [16,18–20,22–26]. All studies have reported less negative chemical shifts (higher resonance frequencies) at lower silica contents and lower average polymerization. This general trend is expected from data on crystalline silicates with known structures: in general, Si sites with fewer bridging oxygens are less shielded. However, detailed interpretations of ^{29}Si MAS results, even of similar spectra obtained from similar composition glasses, have varied greatly. In particular, it is uncertain whether the number of structural species with different numbers of bridging oxygens is equal to, or is greater than, the number of resolvable peaks in the ^{29}Si MAS NMR spectrum.

For example, Murdoch et al. [19] studied binary silicate glasses of mean Q^2 and Q^3 composition. The ^{29}Si MAS spectra of each showed only single, broad peaks, some of which had noticeable shoulders. Linewidths were ascribed to

distributions of up to three silicate species accompanied by bond angle and bond length variations. Network modifying cations with greater cation potential (charge/cation radius) lead to systematically greater linewidths. This suggested that eq. (1) is shifted to the right by smaller, more highly charged cations, in agreement with with long-standing conclusions based on other types of spectroscopy and on thermodynamic data. Two central peaks of approximately equal intensity were observed in $Na_2Si_4O_9$ glass (mean $Q^{3.5}$ composition), and were attributed to well-defined Q^3 and Q^4 sites. It was not clear however, whether this glass consisted of one or two phases.

Several other authors have observed asymmetric and double-peaked ^{29}Si MAS NMR spectra of alkali silicate glasses with both integer and non-integer mean Q^n composition. Interpretations of these results have varied considerably. In several reports, multiple Gaussian curves were fitted to spectra to constrain structural models with statistical distributions of as many as five structural species [18,19,25]; in others, no more than one or two curves were fitted to nearly identical data [16,22,24]. In some cases, the relative abundance of species derived from curve fits may not be accurate or structurally realistic [25], possibly because of different relaxation times for different species, or because of inappropriately chosen lineshapes. To complicate matters, glasses composed mainly of alkaline earth silicates, and most or all aluminosilicate glasses, have only broad, single ^{29}Si MAS NMR peaks, even in compositions where all structural models indicate that two or three species must exist [15,20,23].

Given the variety of interpretations placed on ^{29}Si MAS NMR spectra of glasses, it is clear that the type of information which can be derived from these data is open to some question. We have undertaken this study to better constrain what may and what may not be learned: new results presented here highlight the influences of composition, type of network modifying cation, and relaxation times. A second motivation is more specific: some of the alkali silicate glasses in previous reports showed obvious signs of not being single-phased, homogeneous materials, and thus were not good representatives of the single-phased liquid structure. All glasses synthesized for this study were quenched rapidly and were not annealed. All are optically clear, and are free of crystals at the size (1–2 nm) and abundance (5%) detectable by powder X-ray diffraction.

2. Experimental

Four binary alkali and alkaline earth silicate glasses of non-integer mean Q^n number were synthesized: $K_2Si_4O_9$ and $Na_2Si_4O_9$ (both tetrasilicates, $Q^{3.5}$), and $(CaO)_{0.4}(SiO_2)_{0.6}$ and $(Na_2O)_{0.4}(SiO)_{0.6}$ (both $Q^{2.67}$). A sodium tetrasilicate glass was also made from 95% ^{29}Si enriched SiO_2 to maximize the signal to noise ratio and to facilitate relaxation time measurements.

Glass samples were prepared in approximately 1 g batches from reagent grade oxides and carbonates. The mixtures were heated in sealed platinum capsules to about 100°C above their liquidus temperatures, and quenched by dropping into water. Glasses were then ground, remelted, and requenched to ensure homogeneity. All samples were stored under vacuum to prevent water uptake.

^{29}Si NMR data were collected with a homebuilt Fourier transform spectrometer with an 85 kG superconducting magnet. Most spectra were acquired using "magic angle" spinning rates between 1 and 4 kHz, 45° pulse lengths of 10 μs, and a 50 kHz bandwidth. Delay times of 30 to 60 s were chosen in an attempt to allow complete relaxation between pulses. Rotor spinning speeds were determined by measuring spinning sideband separation. Relaxation time measurements were made using the "progressive saturation" [46] method, and static (non-spinning) spectra were collected using a phase cycled "spin-lock" pulse sequence [46]. ^{29}Si isotropic chemical shifts are referenced by sample exchange to the ^{29}Si resonance of tetramethylsilane (TMS) with ^{1}H decoupling.

The Argonne National Laboratory spectral deconvolution subroutine va02a (modified from a curve-fitting program supplied by B. Mysen) was used to fit the spectra presented here. Gaussian lineshapes were chosen, on the assumption that broad lines in these samples are due to a statistical distribution of some structural parameter. The number of peaks of a given fit was chosen as the number of obvious spectral features (such as clearly resolved peaks and sidebands). To determine the mathematical stability of a fit, several deconvolutions were obtained using different initial conditions for peak locations, widths, and intensities. The estimated error of a fit is a maximum of 5% of peak location and height, and 20% for full width at half maximum (fwhm) intensity and hence for peak area. Central peak widths agree with spinning sideband values. Sidebands, when present, were assigned to the proper central peak on the basis of spacing in chemical shift, and their areas were included when calculating relative abundances of species. A very broad low intensity component seemed to be present in some spectra, but could not be easily deconvoluted. The structural significance of this feature is not yet clear, but its presence decreases the accuracy of fitting of the outer sidebands.

3. Results

3.1. Spectra

In natural abundance and in 95% ^{29}Si enriched $Na_2Si_4O_9$ glass (the latter shown in fig. 1), two broad, overlapping peaks are observed, similar to results obtained by other authors on unenriched material [22] but with a much higher signal to noise ratio. These resonances are ascribed to Q^3 and Q^4 silicate species on the basis of chemical shifts similar to those of crystalline $Na_2Si_2O_5$

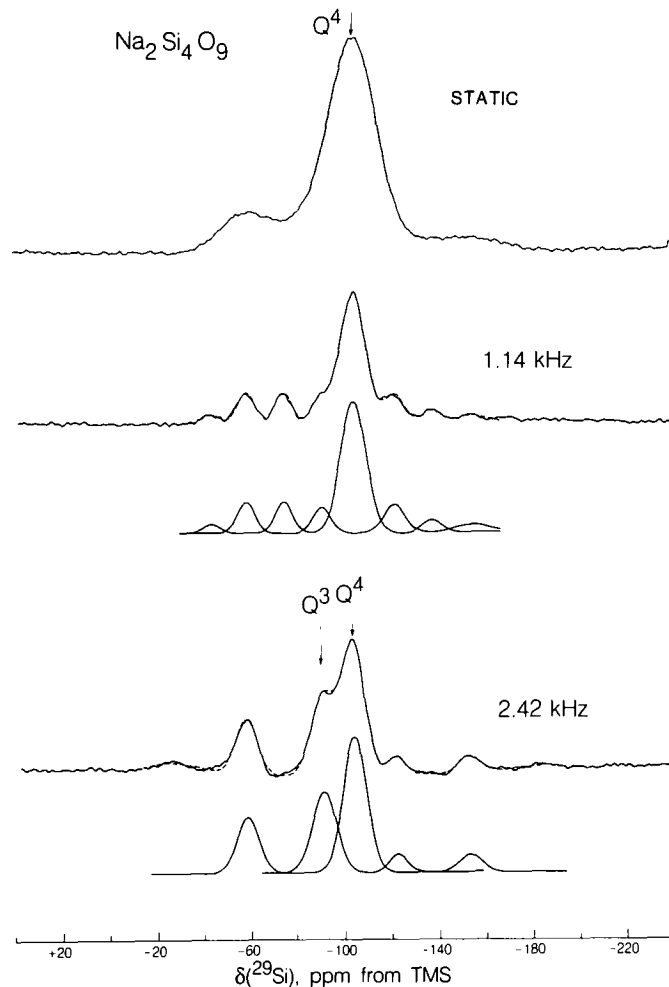Fig. 1. ^{29}Si NMR spectra of 95% ^{29}Si enriched Na$_2$Si$_4$O$_9$ glass. A 45° pulse length of 10 μm, 600 signal averages, and a pulse repeat time of 60 s were used in both. (Top) Spectrum of non-spinning (static) sample, obtained using a phase alternated spin lock pulse sequence. (Middle and Bottom) MAS spectra at moderate (1.14 and 2.42 kHz) sample spinning rates. Experimental data are shown by solid lines and fitted spectra by dashed lines. Individual deconvoluted peaks are shown below spectra. All but the two central peaks are spinning sidebands, illustrating the asymmetry and chemical shift anisotropy of the Q^3 site.

(-98 ppm) and SiO$_2$ (-108 ppm for quartz) [40]. Several spinning sidebands (2–5) are observed for the Q^3 species at moderate spinning speeds (1.2–2.4 kHz), indicating that this site has an asymmetric electron distribution. This result is expected from the geometry of the crystalline analogue [40]. The lack of sidebands associated with the Q^4 site suggests that its local electron distribution has tetrahedral symmetry, again as anticipated from data on crystalline phases [14,41–43].

Presuming that only these two silicate species are abundant enough to strongly influence the shape of the spectrum, deconvolution of the center and lower MAS spectra of $Na_2Si_4O_9$ in fig. 1 yields relative peak areas (table 1) which agree fairly well with the values expected from stoichiometry. However, the presence of small amounts (5–10%) of other species cannot be excluded. The near equality of the two peak areas confirms that they cannot be caused by sub-optical scale phase separation. The shape and position of the metastable solvus in the $Na_2O–SiO_2$ system would permit only a small proportion of a high-silica, Q^4-rich phase to form at this composition [43] and not a 50–50 mixture of phases.

Fitting of the spectra also allows estimation of the chemical shielding anisotropy (CSA) tensor, which can provide more information about the local symmetry of the electron distribution around the probe nucleus and thus about the bonding configuration at the site. Using the method of Herzfield and Berger [42], parameters describing the CSA tensor were obtained from the relative intensities of the spinning sidebands at several spinning speeds. The most accurate quantity which could be ascertained was the magnitude of the anisotropy ($\sigma_{33}–\sigma_{11}$ in table 1) for the glass Q^3 species. The value is similar to that for the analogous site in crystalline $Na_2Si_2O_5$ (−107 ppm, [40]). The asymmetry parameter η, which varies from 0 with perfect uniaxial symmetry to a maximum value of 1 at minimum symmetry, cannot be determined very accurately for the glass with this method because of its insensitivity to certain ranges of data and the uncertainties in deconvolution of the broad, overlapping central peaks. However, η appears to be smaller for the Q^3 site in the glass than in the crystal (0.24, [40]).

A static ^{29}Si NMR spectrum of the 95% isotopicly enriched $Na_2Si_4O_9$ glass was also obtained (fig. 1, top), which resembles the ^{29}Si spectra collected at temperatures just above the glass transition on a metastable melt of the same composition [32,33]. Despite the overlap of the resonances for the Q^3 and Q^4 species, individual CSA tensor patterns can be distinguished. The Q^3 site has approximately axial symmetry with $\sigma_{33} − \sigma_{11} = \pm 110$ ppm. The Q^4 site shows no deviation from tetrahedral symmetry in the static spectrum, as expected from the MAS results.

The MAS spectrum of $K_2Si_4O_9$ glass (fig. 2) is qualitatively similar to that of its sodium analogue: two broad peaks are observed which can be attributed primarily to Q^3 and Q^4 sites. Because of the unlikeliness of phase separation in this system [44] the two resonances must be attributed to different local structures in a homogeneous material, and thus probably represent the structure of the melt at the glass transition. Relative abundances of the two species estimated from a deconvolution into two Gaussian peaks are not, however, consistent with the analyzed composition: the Q^4 sites appear to be under-represented (table 1). This may indicate that the atoms in these sites relax more slowly than those in the Q^3 site. The discrepancy could also be due to real lineshapes which are non-Gaussian.

To examine the effects of large differences in cationic field strength, as well

Table 1
^{29}Si chemical shielding in binary silicate glasses [a]

Nominal composition	Mean speciation	Relative peak areas:			Overall fwhm	Species	σ_{iso}	$\sigma_{33} - \sigma_{11}$ [c]	Deconvoluted fwhm
		Ratio	Expected [b]	Measured					
$(Na_2O)_{0.4}(SiO_2)_{0.6}$	$Q^{2.67}$	Q^2/Q^3	0.74	0.7	20.4	Q^2	−76.3	112±10	7.6
						Q^3	−86.5	113±5	9.8
$(CaO)_{0.4}(SiO_2)_{0.6}$ [d]	$Q^{2.67}$	Q^2/Q^3	0.5	–	19.9	–	−85.8	–	–
$Na_2Si_4O_9$	$Q^{3.5}$	Q^3/Q^4	1.07	1.3	21.5	Q^3	−93.0	112±5	9.8
						Q^4	−105.9	– [e]	11.5
$Na_2Si_4O_9$ (95% ^{29}Si enriched)	$Q^{3.5}$	Q^3/Q^4	1.0	1.0	24.5	Q^3	−92.2	109±10	10.3
						Q^4	−106.4	– [e]	11.7
$K_2Si_4O_9$	$Q^{3.5}$	Q^3/Q^4	0.97	2.0	16.1	Q^3	−95.3	133±15	11.5
						Q^4	−104.8	– [e]	8.9

[a] Data in table are from MAS spectra. Values of σ in ppm relative to TMS. Precision of peak positions is ±0.2 ppm; of fwhm ±0.5 ppm.

[b] Expected areas are shown for comparison only, and are based on composition combined with the very rough approximation that only two species are present in each glass. Wet chemical analyses give the following alkali contents: $(Na_2O)_{0.4}(SiO_2)_{0.6}$, 42.4 wt% Na_2O; $NaSi_4O_9$, 21.0 wt% Na_2O; $K_2Si_4O_9$, 27.8 wt% K_2O. Expected areas for the other two samples are based on weighed-in components.

[c] Errors were estimated from comparison of results from several different spectra for each sample.

[d] For $(CaO)_{0.4}(SiO_2)_{0.6}$ glass, uncertainty in peak maximum is ±0.5 ppm, in fwhm, ±1.5 ppm. Deconvolution into multiple peaks is poorly constrained.

[e] No spinning sidebands are observed that can be linked to the Q^4 peaks, indicating that the symmetry of the sites is high.
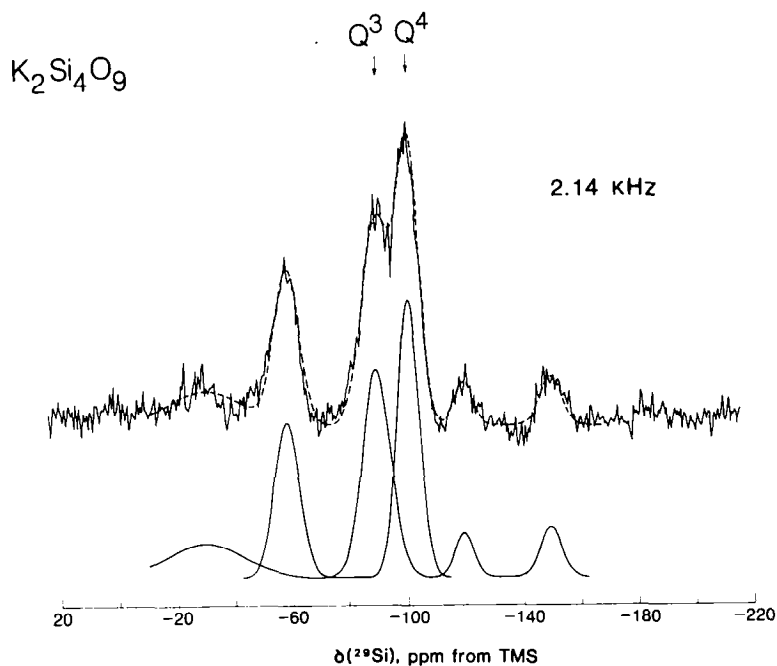
$K_2Si_4O_9$

Q^3 Q^4
↓ ↓

2.14 kHz

20   -20   -60   -100   -140   -180   -220

δ(^{29}Si), ppm from TMS

Fig. 2. ^{29}Si MAS NMR spectrum of $K_2Si_4O_9$ glass. A spinning rate of 2.14 kHz, pulse repeat time of 60 s, and 1200 averaged were used. Symbols as in fig. 1.

as a different range of silica contents, we have collected ^{29}Si MAS NMR spectra of $(Na_2O)_{0.4}(SiO_2)_{0.6}$ and $(CaO)_{0.4}(SiO_2)_{0.6}$ glasses. These have the same stoichiometry and thus the same average state of polymerization $(Q^{2.67})$.
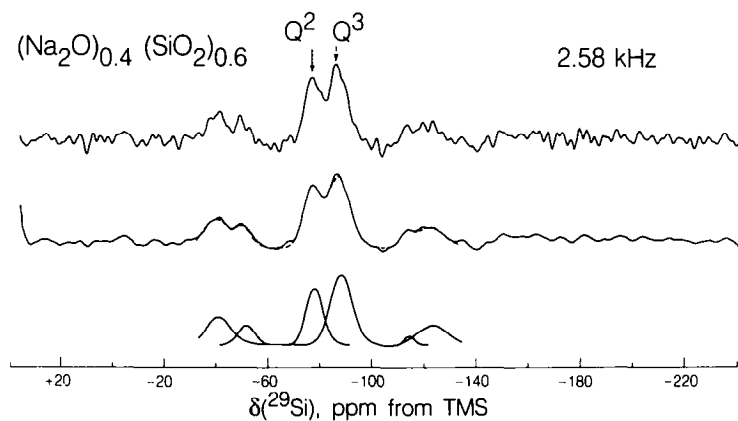
$(Na_2O)_{0.4}$ $(SiO_2)_{0.6}$

Q^2 Q^3
↓ ↓

2.58 kHz

+20   -20   -60   -100   -140   -180   -220

δ(^{29}Si), ppm from TMS

Fig. 3. ^{29}Si MAS NMR spectrum of $(Na_2O)_{0.4}(SiO_2)_{0.6}$ glass. A spinning rate of 2.58 kHz, pulse repeat time of 30 s, and 1200 averages were used. (Top) Experimental data. (Middle) Smoothed data. (Bottom) Deconvoluted smoothed spectrum.
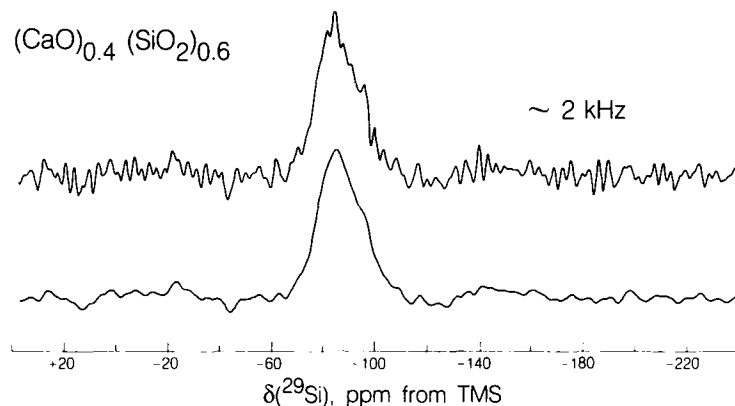
Fig. 4. ^{29}Si MAS NMR spectrum of $(CaO)_{0.4}(SiO_2)_{0.6}$ glass. A spinning rate of approximately 2 kHz, pulse repeat time of 30 s, and 1400 averages were used. Smoothed spectrum is at bottom.

This composition was selected to minimize both the liquidus temperatures and the sodium content (and thus the susceptibility to water absorption).

For the $(Na_2O)_{0.4}(SiO_2)_{0.6}$ glass, two peaks are observed which can be assigned to Q^2 and Q^3 sites (fig. 3). Again, the presence of small amounts of other species cannot be excluded without independent constraints on peak shape. The isotropic chemical shifts (table 1) are in good agreement with those observed in a similar composition glass by Grimmer et al. [16] (-77.7 and -87.3 ppm). The former value is very close to that observed for crystalline Na_2SiO_3 at -76.8 ppm [16]. The width of the deconvoluted Q^3 peak in $(Na_2O)_{0.4}(SiO_2)_{0.6}$ glass is within fitting error of the Q^3 peak width in $Na_2Si_4O_9$ glass (table 1). However, the Q^2 peak is considerably narrower.

The spectrum of $(CaO)_{0.4}(SiO_2)_{0.6}$ glass is rather different: only a single, broad, asymmetric peak is observed. A minor shoulder may be present at about -97 ppm (fig. 4). No unique deconvolution into multiple Gaussian peaks was possible without arbitrary constraints on peak positions or widths. If distinct Q^2 and Q^3 sites are present in this sample with no intermediate structure, other contributions to the peak width (such as variation in intertetrahedral angles) must be much greater than in the sodium analogue.

3.2. Relaxation times

In a solid, relaxation of excited nuclear spin states by transfer of energy to "lattice" (or thermal) energy (spin lattice relaxation) may be a complex process and, in theory, cannot be adequately described by a single relaxation time T_1. Nonetheless, fitting data with a simple function including one or a sum of several exponentials (each with a single value of T_1) is a useful means of characterizing relaxation behavior. The two peaks in the ^{29}Si MAS NMR spectrum of isotopically enriched $Na_2Si_4O_9$ glass were found to have the same

relaxation rate when the data were fitted with a single T_1 [(25 ± 1)s]. A better fit was obtained with two T_2 values. A short T_2, accounting for 20–30% of the observed signal, had values of about 4 s for the Q^3 site and 1 s for the Q^4 site. These values are probably the same within the error of the fit. A second, longer T_2 was found with a value of ≈ 25 s for both sites. Both peaks in the spectrum for the unenriched glass of the same composition also have the same T_1 values in single parameter fits [(27 ± 7) s and (35 ± 10)s respectively].

4. Discussion and conclusions

Murdoch et al [19] made a quantitative comparison of alkali and alkaline earth silicate glass structure using ^{29}Si MAS NMR. Extending that work, we have confirmed here that double peaks seen in spectra of sodium and potassium silicate glasses of noninteger mean Q^n composition are present even when the materials are definitely homogeneous and single-phased. As other authors have assumed [16,18,19,22,25], we interpret these peaks as resulting from the presence of two distinct silicate species with different numbers of non-bridging oxygen atoms. The observed isotropic ^{29}Si chemical shifts are consistent with the conclusion that the most abundant species are those which are predicted by stoichiometry alone (e.g. $Q^3 + Q^4$ in a glass with mean $Q^{3.5}$ composition). The ^{29}Si NMR spectra cannot eliminate the possibility of small but significant numbers of other species (at less than the 5–10% level) without assumptions about peak shapes. This type of data can therefore be used to constrain structural models, but not to choose among them.

This conclusion is particularly evident when comparison is made between alkali and alkaline earth silicate glasses. In the latter, single, broad peaks are observed even at noninteger mean Q^n compositions. Hence, a simple assumption of a one-to-one correspondence between resolvable NMR peaks and discrete species is not likely to be valid. This conclusions is supported by the fact that the total widths of ^{29}Si NMR resonance for glasses (including alkali silicates) often span the chemical shift ranges observed for three or more groups of minerals, each of which has a different state of silicate polymerization.

The broad peaks observed for alkaline earth silicate glasses could conceivably be due to a continuous range in the number of bridging oxygens, with distorted sites having bonding characteristics between those of the well-defined tetrahedra of silicate crystals. We consider this to be unlikely, however, as Raman spectra on alkaline earth silicate glasses show partially resolved peaks which have been attributed to Si–O stretching motions of distinct, integer Q^n species [3,8]. On the other hand, the distinction between "bridging" and "non-bridging" oxygens does decrease as the field strength of the network modifying cation increases. The local electronic structure at silicon sites with varying numbers of bridging oxygen atoms may thus also become less distinct.

Variations in structural parameters other than the populations of Q^n

species must have an important contribution to the ^{29}Si MAS NMR linewidth [14,16,19,22,24]. Data on SiO_2 glass [14,19,48] best illustrates this conclusion: because no network modifying cations are present, all silicon atoms must be in either Q^4 or in defect sites. A broad peak is nonetheless observed.

In glasses of more complex composition, the additional variable of polymer speciation is present. The distribution of bond angles and lengths, and of Q^n species are all inter-related. The variance (i.e. the width of the distribution) in each of these variables may be increased by stronger interactions of network modifying cations with the oxygen atoms of the structure, giving rise to the observed increase in NMR linewidth from glasses with large, low-charge cations to those with small, high charge cations. The distinction observed between different Q^n species seen in the ^{29}Si NMR spectra of alkali silicate glasses is lost in the alkaline earth glasses for the same reason.

^{29}Si NMR spectroscopy of glasses can provide new information about the local symmetry of structural sites in glasses, through determination of the chemical shift anisotropy (CSA). In the sodium silicate glasses, Q^2 and Q^3 sites have similar CSA magnitudes $(\sigma_{33} - \sigma_{11})$ which are within the range typical for tetrahedral silicon in crystals. The CSA for Q^4 species in several glass compositions, as in crystalline framework silicates, is too small to be measured. This indicates that tetrahedrally symmetrical electron distributions surround Q^4 silicon nuclei. A distribution of bond angles and corresponding bond lengths must occur and contributes to the linewidth, in agreement with Raman spectroscopic data [8]. In $Na_2Si_4O_9$ glass, Q^3 sites appear to have close to uniaxial symmetry, implying that sites have three equal silicon-bridging oxygen bond distances and three equal O–Si–O bond angles. This is true locally, and is *not* the result of an average over sites with a wide range of distortions (preliminary results for $Na_2Si_2O_5$ glass suggest less symmetry in this composition). This finding is different from that for crystalline alkali silicates [40], in which Q^3 sites are generally not axially symmetric because of the constraints of low symmetry, long-range crystallographic order. The lack of such constraints in the melt allows the local structure to relax to higher symmetry.

Relaxation time data may eventually lead to further understanding of glass structure, if the relaxation processes can be characterized. In $Na_2Si_4O_9$ glass, the Q^3 and Q^4 sites appear to have about the same spin lattice relaxation behavior in the MAS experiment. However, in $K_2Si_4O_9$ glass (table 1), the observed relative peak areas suggest that the Q^4 site in this material has a considerably longer T_1. A possible explanation for these observations is a contribution to relaxation by dipole–dipole coupling between silicon atoms and quadrupolar alkali cations. This coupling should be much smaller for potassium than for sodium, as the gyromagnetic ratio is only one sixth as great. The involvement of quadrupolar alkali cations in ^{29}Si relaxation is also supported by the very long relaxation times observed for pure SiO_2 glass: here only very weak CSA interactions, and paramagnetic or proton-containing impurities, are available to allow relaxation [45].

In conclusion, it is difficult to uniquely constrain any single structural variable in silicate glasses by ^{29}Si NMR. However, the sensitivity of the technique to geometrical changes and the one-to-one correspondence between signal intensity and number of resonating nuclei can make NMR data very valuable for constraining specific structural models. In particular, observed peak shapes and widths may eventually provide a good measure of *all* contributions to the configurational entropy of a glass.

Note added in proof: Grimmer and Muller (Monatsh. Chem. 117 (1986) 799) have recently published a careful ^{29}Si MAS NMR study on a series of potassium silicate glasses collected at a relatively low frequency where spinning sidebands could be eliminated. In these samples, relaxation times appeared to be short enough to allow good correlation between relative peak areas and composition, assuming that just two species were present. It is important to note that as pointed out in ref. [19], formation of additional species is more probable in glasses with cations that are smaller or more charged than K.

References

[1] B.O. Mysen, D. Virgo and F.A. Seifert, Rev. Geophys. 20 (1982) 353.

[2] D.W. Matson, S.K. Sharma and J.A. Philpotts, J. Non-Cryst. Solids 58 (1983) 323.

[3] P. McMillan and B. Piriou, J. Non-Cryst. Solids 53 (1982) 279.

[4] S.A. Brawer and W.B. White, J. Chem. Phys. 63 (1975) 2421.

[5] K. Kusabiraki and Y. Shiraishi, J. Non-Cryst. Solid 44 (1981) 365.

[6] I.A. Harris and P.J. Bray, Phys. Chem. Glasses 21 (1980) 156.

[7] A. Navrotsky, K.L. Geisinger, P. McMillan and G.V. Gibbs, Phys. Chem. Miner. 11 (1985) 284.

[8] P. McMillan, Amer. Mineral. 69 (1984) 622.

[9] M. Taylor and G.E. Brown Jr, Geochim. Cosmochim. Acta 43 (1979) 61.

[10] M. Taylor and G.E. Brown Jr, Geochim. Cosmochim. Acta 43 (1979) 1467.

[11] Y. Waseda, The Structure of Non-Crystalline Solids (McGraw–Hill, New York, 1980).

[12] B.H.W.S. deJong and G.E. Brown Jr, Geochim. Cosmochim. Acta 44 (1980) 1627.

[13] D.A. McKeowan, G.A. Waychunas and G.E. Brown Jr, J. Non-Cryst. Solids 74 (1985) 336.

[14] E. Dupree and R.F. Pettifer, Nature 308 (1984) 523.

[15] E. Lippmaa, A. Samoson, M. Mägi, R. Teeäär, J. Schraml and J. Götz, J. Non-Cryst. Solids 50 (1982) 215.

[16] A.-R. Grimmer, M. Magi, M. Hahnert, H. Stade, A. Samoson, W. Wieker and E. Lippmaa, Phys. Chem. Glasses 25 (1984) 105.

[17] B.H.W.S. deJong, C.M. Schramm and V.E. Parziale, Geochim. Cosmochim. Acta 47 (1983) 1223.

[18] C.M. Schramm, B.H.W.S. deJong and V.E. Parziale, J. Amer. Chem. Soc. (1984) 4396.

[19] J.B. Murdoch, J.F. Stebbins and I.S.E. Carmichael, Amer. Mineral. (1985) 332.

[20] R.J. Kirkpatrick, K.A. Smith, R.A. Kinsey and E. Oldfield, Trans. Am. Geophys. Union 63 (1982) 1140.

[21] R.J. Kirkpatrick, R.A. Kinsey, K.A. Smith, D.M. Henderson and E. Oldfield, Amer. Mineral. 70 (1985) 106.

[22] R. Dupree, D. Holland, P.W. McMillan and R.F. Pettifer, J. Non-Cryst. Solids 68 (1984) 399.

[23] G. Engelhardt, M. Nofz, K. Forkel, F.G. Wihsmann, M. Mägi, A. Samoson and E. Lippmaa, Phys. Chem. Glasses 26 (1985) 157.

[24] C.N.R. Rao, J.M. Thomas, J. Klinowski, U. Selvaraj, K.J. Rao, G.R. Millward and S. Ramdas, Angew. Chem. Int. Ed. English 24 (1985) 61.

[25] U. Selvaray, K.J. Rao, C.N.R. Rao, J. Klinowski and J.M. Thomas, Chem. Phys. Lett. 114 (1985) 24.

[26] P.J. Bray, A.E. Geissberger, F. Bucholtz and I.A. Harris, J. Non-Cryst. Solids 52 (1982) 45.

[27] T.L. Weeding, B.H.W.S. deJong, W.S. Veeman and B.G. Aitken, Nature 318 (1985) 352.

[28] C.A. Fyfe, G.C. Gobbi and A. Putnis, J. Amer. Chem. Soc. 108 (1986) 3218.

[29] C.A. Fyfe, Solid State NMR for Chemists (CFC Press, Guelph, Ontario, 1983).

[30] R.K. Harris and C.T.G. Knight, J. Chem. Soc., Faraday Trans. (1983) 1525.

[31] E. Lippmaa, M. Mägi, A. Samoson, G. Engelhardt and A.-R. Grimmer, J. Amer. Chem. Soc. 102 (1980) 4889.

[32] J.F. Stebbins, E. Schneider, J.B. Murdoch, I.S.E. Carmichael and A. Pines, Rev. Sci. Instr. 57 (1986) 39.

[33] J.F. Stebbins, J.B. Murdoch, E. Schneider, I.S.E. Carmichael and A. Pines, Nature 314 (1985) 250.

[34] A.-R. Grimmer, F. von Lampe, M. Mägi and E. Lippmaa, Monatsh. Chemie 115 (1984) 561.

[35] J.V. Smith and C.S. Blackwell, Nature 303 (1983) 223.

[36] A.-R. Grimmer, F. von Lampe, M. Mägi and E. Lippmaa, Monatsh. Chemie 114 (1983) 1053.

[37] G. Engelhardt and R. Radeglia, Chem. Phys. Lett. 108 (1984) 271.

[38] S. Ramdas and J. Klinowski, Nature 308 (1984) 521.

[39] A.-R. Grimmer and R. Radeglia, Chem. Phys. Lett. 106 (1984) 262.

[40] K.A. Smith, R.J. Kirkpatrick, E. Oldfield and D.M. Henderson, Amer. Mineral 68 (1983) 1206.

[41] M.M. Maricq and J.S. Waugh, J. Chem. Phys. 70 (1979) 3300.

[42] J. Herzfield and A.E. Berger, J. Chem. Phys. 73 (1980) 6021.

[43] W. Haller, D.H. Blackburn and J.H. Simmons, J. Am. Chem. Soc. 57 (1974) 120.

[44] M. Tomozawa, Phys. Chem. Glasses 13 (1972) 161.

[45] L.F. Gladden, T.A. Carpenter and S.R. Elliot, Phil. Mag. B53 (1986) L 81.

[46] E. Fukushima and S.B.W. Roeder, Experimental Pulse NMR (Addison-Wesley, Reading, Ma, 1981).